

Observer-based adaptive super-twisting fast terminal sliding mode control for attitude of quadrotor with mismatched disturbances

Proc IMechE Part I:
J Systems and Control Engineering
2025, Vol. 239(5) 881–891
© IMechE 2025
Article reuse guidelines:
sagepub.com/journals-permissions
DOI: 10.1177/09596518241300676
journals.sagepub.com/home/pii
 Sage

Shuzhen Han¹, Shanshan Zhang² , Jianfei Li³ and Zhanshan Zhao³

Abstract

This paper presents an adaptive super-twisting fast terminal based on disturbance observer sliding mode control method for the attitude tracking of a quadrotor unmanned aerial vehicle in the presence of mismatched disturbances. The attitude tracking controller is formulated based on the introduced adaptive super-twisting technique. The utilization of dynamically adaptive gains in the controllers enhances the system's robustness while reducing chattering effects. Additionally, a non-singular fast terminal sliding surface based on finite-time disturbance observer is defined. This approach effectively addresses the issue of mismatched disturbances while accelerating the convergence of tracking error. The stability analysis of the closed-loop system is established employing Lyapunov function. Finally, the effectiveness and success of the proposed method are validated through simulation and experimental results, with further comparisons to other techniques in terms of tracking performance and robustness.

Keywords

Quadrotor UAV, adaptive control, super-twisting algorithm, disturbance observer, mismatched disturbance, fast terminal control

Date received: 8 November 2023; accepted: 18 October 2024

Introduction

The quadrotor is a typical type of unmanned aerial vehicles (UAVs) that incorporates a unique design with four rotors instead of the traditional single rotor used in helicopters.^{1,2} Due to their simple structure, convenient operation, low cost, vertical takeoff and landing capabilities and hover ability, quadrotors have gained significant attention from scholars in the last years.³ Quadrotors have been widely used in various scenarios, such as topographic exploration,⁴ military reconnaissance,⁵ aerial search and rescue,⁶ aerial photography,⁷ air pollution detection,⁸ power inspection and agricultural service.^{9,10} A quadrotor aircraft represents a complex and highly nonlinear system with strong coupling, which poses numerous challenges in effectively controlling its attitude. Moreover, the system faces parameter uncertainties and external disturbances, such as disturbance from atmosphere, wind forces and model uncertainties, further increasing the complexity of control.

Thus, a range of control strategies have been explored in the literature to achieve accurate attitude

control for quadrotors, including backstepping technique,¹¹ H_∞ control,¹² fuzzy control,¹³ sliding mode control (SMC)^{14,15} and others. SMC is acknowledged as a highly effective nonlinear control method that exhibits prominent advantages, including strong robustness and disturbance rejection.¹⁶ Thanks to these notable features, the SMC technique has found application across various dynamical systems in some papers. Considering robustness of a quadrotor, In Chen et al.,¹⁷ the paper combines the nonlinear extended state observer controller with recursive SMC to control the attitude of the UAV and track the desired trajectory. In Nettari

¹School of Mechanical Engineering, Tiangong University, Tianjin, China

²School of Computer Science and Technology, Tiangong University, Tianjin, China

³School of Software, Tiangong University, Tianjin, China

Corresponding author:

Zhanshan Zhao, School of Software, Tiangong University, No. 399 Binshui Road, Xiqing District, Tianjin, 300387, China.
Email: zhzhsh127@163.com

et al.,¹⁸ an adaptive backstepping SMC is designed to stabilize the quadrotor system in the presence of uncertain system parameters. A trajectory tracking control law based on a state observer and an improved event-triggered strategy¹⁹ is presented for the control of uncertain manipulators. By reducing the number of control updates and saving communication resources, the proposed approach improves control performance and stability. In Singh et al.,²⁰ this paper designs a combined scheme using the robust backstepping SMC and adaptive neural network to achieve asymptotic control of attitude and altitude of the aircraft.

It is worth noting that due to the inherent discontinuity of SMC can result in chattering. This occurrence potentially impedes its practical application. For the problem of high-frequency chattering, a set of continuous sliding mode controllers known as super-twisting algorithm has been developed in Levant.²¹ Super-twisting deals with chattering without affecting the robustness of the system and provides higher tracking accuracy in finite time. In Derafa et al.,²² this paper proposes a super-twisting controller algorithm and effectively applies it to quadrotor, enabling the attitude tracking error of the quadrotor UAV to converge to zero. It indicates that controllers based on super-twisting are suitable for attitude control of quadrotor. Moreover, a modified super-twisting control is proposed in Kahouadji et al.,²³ in which the discontinuous control function smoothed through integration in classical super-twisting algorithm is substituted with a continuous control function. This method can further attenuate the chattering phenomenon and achieve more accurate tracking.

The main disadvantage of the super-twisting controller is that it requires knowledge of the upper bound of the disturbances, which is often difficult to achieve in many practical situations. Overestimating the bounds of disturbances can lead to excessive gains. Excessive gains can cause chattering and instability in the system. In addition, high gains may cause the controller output to saturate, limiting its ability to further respond to errors or disturbances.²⁴ To prevent the overestimation of control gains that exacerbates chattering, incorporating adaptive algorithms into SMC, offers an efficient approach to tackle the situations where disturbance boundaries exist but are unknown.²⁵ A hybrid control approach combining the adaptive method and super-twisting²⁶ is proposed to improve the resistance to disturbances of the quadrotor. In Xu et al.,²⁷ this paper designs a trajectory tracking controller for a quadrotor UAV by incorporating event-triggering mechanisms and an active disturbance rejection technique to mitigate the effects of unknown disturbances. An adaptive gain²⁸ to address situations where disturbance boundaries exist but are unknown. The gain is gradually increased until the sliding mode is achieved, and then the gain is fixed at that value to ensure the desired sliding mode effect is attained within a certain range. The drawback of this approach is that the adaptive gains can be only increased. In Shtessel et al.,²⁹ this paper

provides a dynamic gain that can be increased or decreased for formulating a super-twisting sliding mode controller for the an electropneumatic actuator. These adaptive methods ensure that the sliding variable converges to a neighborhood of zero without greatly overestimating the gain. Inspired by Kahouadji et al.²³ and Shtessel et al.,²⁹ this paper proposes an adaptive super-twisting sliding mode control (ASTSMC), where the control gains can dynamically adapt to various uncertainties, even in situations where the upper bound of disturbances is present but unknown.

On the basis of ensuring robustness in attitude control, it is also necessary to further improve the convergence speed to achieve more efficient flight control and perform more complex tasks, especially for quadrotor UAVs. Rapid and precise attitude control contributes to stable and accurate flight maneuvers, thereby enhancing system performance to meet the requirements of various application scenarios. However, SMC does not ensure the fast convergence of the trajectories of the quadrotor. Thus, a terminal sliding mode (TSMC) control is proposed, which adopts a nonlinear sliding surface. However, the traditional TSMC suffers from a singularity problem if the initial conditions are not given properly. To address the singularity problem and ensure fast convergence, an advanced non-singular fast terminal sliding mode control³⁰ is introduced. This control method ensures rapid convergence not only near the equilibrium point but also at larger distances from it, enabling faster and more efficient attainment of the desired state values.

The feedback control methods mentioned above typically adopt an indirect suppression approach to handle system uncertainties, which tends to be conservative in performance and lacks rapid response, making it difficult to completely eliminate the impact of uncertainties. In order to better address the chattering issue caused by sliding mode robustness switching, researchers have proposed introducing compensation mechanisms into the controller to offset the effects of uncertainties in the system. Therefore, disturbance observers have emerged as an effective strategy for mitigating chattering. Disturbance observers are able to estimate real time disturbances in the system and incorporate the estimated values as compensation terms into the controller to counteract the effects of uncertainties. Through this approach, the disturbances in the system can be directly compensated, reducing the magnitude of chattering. A non-singular terminal sliding mode controller³¹ with a disturbance observer for underactuated unmanned surface vessels, overcoming external environmental disturbances. In Luo and Liu³², this paper designs a nonlinear disturbance observer to estimate complex external disturbances and integrated it with nonlinear fractional terminal control to achieve trajectory tracking for underactuated underwater robots. Disturbance observers have emerged as an effective compensation strategy to directly mitigate the impact of uncertainties and external disturbances in

controlled systems, while preserving the performance of the original control method. This makes them highly valuable in practical applications. Uncertainties arising from factors such as model uncertainties, mechanical component wear, and sensor errors in quadrotor UAVs can result in uncertain disturbances. These disturbances, known as unmatched disturbances, cannot be effectively compensated for by control methods, resulting in significant impacts on the performance and stability of the UAV. To address this issue, researchers have focused on incorporating disturbance observers to estimate and compensate for these unmatched disturbances, with the goal of enhancing control performance and stability. A continuous nonsingular terminal sliding mode control method³³ is proposed to address the problem of unmatched disturbances. By introducing a finite-time disturbance observer and designing a novel nonlinear dynamic sliding surface, the proposed method achieves stable finite-time convergence. In Nguyen et al.,³⁴ this paper presents a novel approach to finite-time sliding mode attitude control using a multivariable disturbance observer. By incorporating a multivariable disturbance observer and designing a terminal sliding manifold, the proposed method enables the tracking of desired attitude commands and ensures high-precision performance. Based on the analysis of the above literature, it can be observed that there is relatively limited research on the problem of unmatched disturbances in quadrotor UAVs. Most of the existing control methods are only sensitive to matched disturbances and cannot effectively suppress mismatched disturbances acting on channels different from the control inputs.

Inspired by the aforementioned studies, this paper proposes an observer-based adaptive super-twisting non-singular fast terminal sliding mode control (ASTFTSMC) for quadrotor systems subject to matched and mismatched disturbances. The ASTSMC dynamically adjusts gains to reduce chattering induced by control laws, thereby enhancing control performance. Furthermore, the observer-based fast terminal technique is combined with ASTSMC to compensate for mismatched disturbances using finite-time disturbance observers, preserving control performance and further improving convergence efficiency and disturbance rejection. The main contributions of this paper are as follows:

- Considering the dynamical equations of a quadrotor system with three degrees of freedom subjected to uncertain bounded matched and mismatched disturbances.
- An ASTSMC is proposed for the attitude control problem of a quadrotor with bounded but unknown time-varying disturbances. The value of the dynamic gain in the ASTSMC method changes with the variations of disturbances to ensure the convergence of the sliding surface within a specified range. This approach avoids excessive estimation of

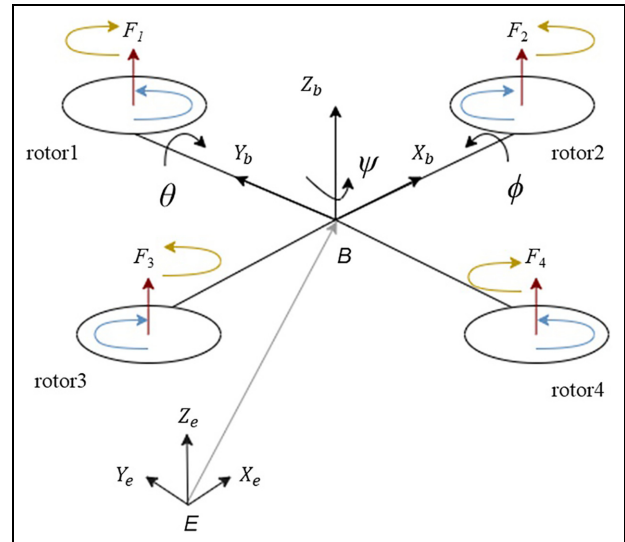


Figure 1. Quadrotor UAV configuration.

the gain, reduces the magnitude of the controller, and effectively suppresses oscillations when encountering time-varying disturbances.

- For the attitude control problem of quadrotor aircraft with both matched and mismatched disturbances, a novel observer-based fast terminal sliding mode method is proposed. A new fast terminal sliding surface is designed to incorporate the estimation errors, ensuring finite-time convergence in the presence of mismatched disturbances. This feature is of utmost significance as in certain control missions, quadrotor systems need to operate safely and stably in highly disturbed environments.

This paper is organized as follows: In Section “Quadrotor dynamics model,” we introduce the attitude dynamics model of the quadrotor. In Section “Attitude controller design,” we design the ASTFTSMC based on observer and analyze the stability of the closed-loop system. Section “Simulation” presents the simulation results of the proposed method and its comparison with other methods. Finally, the primary conclusions of this paper are provided in Section “Conclusion.”

Quadrotor dynamics model

The quadrotor is comprised of a rigid cross frame with four rotors, each equipped with propellers. Figure 1 illustrates a graphical depiction of the quadrotor. The quadrotor is subjected to two reference frames: frame $E = (X_e, Y_e, Z_e)$, which is an earth-fixed inertial frame, and frame $B = (X_b, Y_b, Z_b)$, which is a body-fixed frame. In addition, the body-fixed frame of the quadrotor is situated at its center of mass. The attitude dynamical system can be expressed by Euler angles $\Theta = [\phi, \theta, \psi]^T$, where ϕ is the roll angle around the x-axis, θ is the pitch angle around the y-axis, and ψ is the

yaw angle around the z-axis. The angular velocities and accelerations are provided respectively by $\dot{\Theta} = [\dot{\phi}, \dot{\theta}, \dot{\psi}]^T$ and $\ddot{\Theta} = [\ddot{\phi}, \ddot{\theta}, \ddot{\psi}]^T$.

The attitude of the quadrotor is governed by control torques, which are combined with the forces generated by the four rotors F_1, F_2, F_3 , and F_4 . Γ is employed to counteract the gravitational force and enable vertical motion for a quadrotor with 6 degrees of freedom.

The model of the quadrotor attitude can be given by Kahouadji et al.²³ and Labbadi and Cherkaoui³⁵:

$$\ddot{\Theta} = [J\Psi(\Theta)]^{-1}[U - N(\Theta, \dot{\Theta})\dot{\Theta}] + d \quad (1)$$

where J represents the inertia matrix, U is the control torques, d denotes external matched disturbances, $\Psi(\Theta)$ and $N(\Theta, \dot{\Theta})$ are expressed as

$$\Psi(\Theta) = \begin{bmatrix} 1 & 0 & -\sin(\theta) \\ 0 & \cos(\phi) & \sin(\phi)\cos(\theta) \\ 0 & -\sin(\phi) & \cos(\phi)\cos(\theta) \end{bmatrix};$$

$$N(\Theta, \dot{\Theta}) = -J\Psi(\Theta)\dot{\Psi}^{-1}(\Theta)\Psi(\Theta) - K[J\Psi(\Theta)\dot{\Theta}]\Psi(\Theta)$$

Remark 1. Three angles are constrained within the range $(\phi: -\frac{\pi}{2} < \phi < \frac{\pi}{2})$, $(\theta: -\frac{\pi}{2} < \theta < \frac{\pi}{2})$ and $(\psi: -\pi < \psi < \pi)$. This limitation implies that acrobatic maneuvers are prohibited.

The operator $K[\gamma]$ for a vector $\gamma = [\gamma_1, \gamma_2, \gamma_3]^T$ is provided as:

$$K[\gamma] = \begin{bmatrix} 0 & -\gamma_3 & \gamma_2 \\ \gamma_3 & 0 & -\gamma_1 \\ -\gamma_2 & \gamma_1 & 0 \end{bmatrix}.$$

Taking into account the symmetry of the system, J can be estimated as $J = \text{diag}[J_{xx}, J_{yy}, J_{zz}]$, then the control inputs $[\Gamma, U]$ are determined as:

$$\begin{bmatrix} \Gamma \\ u_\phi \\ u_\theta \\ u_\psi \end{bmatrix} = \begin{bmatrix} K_f & K_f & K_f & K_f \\ 0 & -lK_f & 0 & lK_f \\ -lK_f & 0 & lK_f & 0 \\ K_t & K_t & K_t & K_t \end{bmatrix} \begin{bmatrix} V_1 \\ V_2 \\ V_2 \\ V_2 \end{bmatrix} \quad (2)$$

l represents the distance between the rotors and the center of the quadrotor airframe, V_i is the voltage input generated by rotor i and (K_f, K_t) correspond to the thrust and drag that characterize the aerodynamics of the propellers.

The state vectors are defined as:

$$x_1 = \Theta, x_2 = \dot{\Theta}$$

The dynamic model is reformulated using the state-space format as follows:

$$\begin{cases} \dot{x}_1 = x_2 + d_1(t) \\ \dot{x}_2 = f(x, t) + g(x, t)U + d_2(t) \end{cases} \quad (3)$$

where $d_1(t) = [d_{1\phi}, d_{1\theta}, d_{1\psi}]^T$ and $d_2(t) = [d_{2\phi}, d_{2\theta}, d_{2\psi}]^T$ are considered as mismatched disturbance vector and matched disturbance vector, the control input is $U = [u_\phi, u_\theta, u_\psi]$, $f(x, t)$ is given by

$$f(x, t) = -[J\Psi(\Theta)]^{-1}N(\Theta, \dot{\Theta})\dot{\Theta} \quad (4)$$

and $g(x, t)$ is defined as

$$g(x, t) = [J\Psi(\Theta)]^{-1} \quad (5)$$

In our research, the attitude model is based on the following assumptions refer to Kahouadji et al.²³ and Lei et al.³⁶:

Assumption 1. The desired trajectories and their first and second time derivatives are bounded.

Assumption 2. The signals Θ and $\dot{\Theta}$ can be measured or estimated by on-board sensors.

Lemma 1.²² For three variables $n_1(t)$, $n_2(t)$ and $n_3(t)$, the subsequent inequality is valid as

$$(n_1^2(t) + n_2^2(t) + n_3^2(t))^{\frac{1}{2}} \leq |n_1(t)| + |n_2(t)| + |n_3(t)|.$$

Attitude controller design

In this section, the objective is to design a controller to guarantee the convergence of the attitude trajectories.

Before starting, we formulate the subsequent assumption.

Assumption 3. The sliding variable $s = s(x, t) \in \mathbb{R}$ is formulated to attain desirable dynamics for system (3) when $s(x, t) = 0$. Moreover, system (3) possesses a relative degree of one concerning the sliding variable.

Assumption 4. The time derivative of the disturbance d_1 and d_2 are bounded for $t \geq 0$ with unknown boundaries.

To mitigate the influence of disturbances, the finite-time observer³³ can be employed to approximate the disturbances.

$$\begin{aligned} \dot{z}_0^i &= v_0^i + f_i(x, u), \dot{z}_1^i = v_1^i, \dots, \dot{z}_{n-i+1}^i = v_{n-i+1}^i \\ v_0^i &= -\lambda_0^i L_i^{\frac{1}{n-i+2}} |z_0^i - x_i|^{\frac{n-i+1}{n-i+2}} \text{sgn}(z_0^i - x_i) + z_1^i, \\ v_j^i &= -\lambda_j^i L_i^{\frac{1}{n-i+2-j}} |z_j^i - v_{j-1}^i|^{\frac{n-i+1-j}{n-i+2-j}} \text{sgn}(z_j^i - v_{j-1}^i) + z_{j+1}^i, \\ v_{n-i+1}^i &= -\lambda_{n-i+1}^i L_i \text{sgn}(z_{n-i+1}^i - v_{n-i}^i), \\ \hat{x}_i &= z_0^i, \hat{d}_i = z_1^i, \hat{d}_i = z_2^i, \dots, \hat{d}_i^{[n-i]} = z_{n-i+1}^i, \end{aligned} \quad (6)$$

where $i = 1, 2, \dots, n$ and $j = 1, 2, \dots, n - i + 1$, $\lambda_j^i > 0$ is the observer coefficients, and $\hat{x}_i, \hat{d}_i, \hat{\dot{d}}_i, \hat{d}_i^{[n-i]}$ are the estimates of real value of state variable and disturbance. The tracking errors and the second order derivatives of e , denoted by e and \dot{e} , are defined as follows:

$$e = x_1 - x_{1d}, \dot{e} = \dot{x}_1 - \dot{x}_{1d}$$

where $x_{1d} = [\phi_d, \theta_d, \psi_d]^T$ and $\dot{x}_{1d} = [\dot{\phi}_d, \dot{\theta}_d, \dot{\psi}_d]^T$ denote the desired state vector and its time derivative, respectively. An non-singular fast terminal sliding surface based on the finite-time DO is defined as follows:

$$\begin{aligned} s &= \dot{e} + e_1^1 + \lambda e^{1/a} + qe \\ &= \tilde{x}_2 + \lambda \tilde{x}_1^{1/a} + q\tilde{x}_1 \end{aligned} \quad (7)$$

where $\lambda \in R^{3 \times 3}$, $q \in R^{3 \times 1}$ and $0 < a = \frac{z}{y} < 1$, $0 < z < y$ are odd numbers, $\tilde{x}_1 = x_1 - x_{1d}$, $\tilde{x}_2 = \dot{x}_1 - \dot{x}_{1d}$, the proposed controller is expressed as:

$$\begin{aligned} U &= [J\Psi(\Theta)]\{[J\Psi(\Theta)]^{-1}N(\Theta, \dot{\Theta}) - \hat{d}_2 - v_1^1 + \tilde{x}_{1d} \\ &\quad - \lambda\left(\frac{1}{a}\right)e_1^{(1/a-1)}(x_2 + \hat{d}_1 - \dot{x}_{1d}) - q(x_2 + \hat{d}_1 - \dot{x}_{1d}) \\ &\quad - K_1|s|^{\rho_1}\text{sign}(s) - \omega\} \end{aligned} \quad (8)$$

where $\frac{1}{2} < \rho_1 < 1$, $K_1 = [K_{1\phi}, K_{1\theta}, K_{1\psi}]$ denote the adaptive gains and ω represent the states of the super-twisting controller defined as:

$$\dot{\omega} = K_2|s|^{\rho_2}\text{sign}(s) \quad (9)$$

where $\rho_2 = 2\rho_1 - 1$, $K_2 = [K_{2\phi}, K_{2\theta}, K_{2\psi}]$ are the adaptive positive gains, and the adaptive laws are provided as:

$$\dot{K}_1(t) = \begin{cases} \omega_1 \sqrt{\frac{1}{2}} \text{sign}(|s(t)| - \mu), K_1(t) > K_m \\ \eta, K_1(t) \leq K_m \end{cases} \quad (10)$$

and

$$K_2 = 2\rho_1 \epsilon K_1 \quad (11)$$

where $\omega_1, l_1, \mu, \eta, \epsilon$ and K_m are the adjustable positive parameters.

Theorem 1. Given the sliding mode surface (7), the system (19) is stable for any initial value $s(0)$ if the subsequent equation is satisfied:

$$K_1 > \frac{2\epsilon + \rho_1 \epsilon}{\rho_1 \theta} + \frac{[\rho_1(\theta + 4\epsilon^2)]^2}{4\rho_1^2 \epsilon \theta} \quad (12)$$

where ϵ and θ are arbitrary positive constants. Under the action of the ASTFTSMC structure (8)-(12), the sliding mode system will converge to the origin in finite time t_f , where

$$t_f \leq \frac{\left(|s(0)|^{2\rho_1}(\theta + 4\epsilon^2) - 4\epsilon\bar{\omega}(0)|s(0)|^{\rho_1}\text{sign}(s(0)) + \bar{\omega}^2(0)\right)^{1-\epsilon}}{r(1-\epsilon)}$$

in which r is contingent upon ϵ and θ .

Theorem 1. For system (3) with the proposed non-singular fast terminal sliding surface based on the finite-time DO (7), if the new NFTSMC law is designed (8), then the system output will converge to zero in finite time. Observe-based sliding mode surface design ensures convergence.

Proof 1. According to (7), (8), (9), one obtains that

$$\begin{aligned} \dot{s} &= -e_1^2 - \lambda \frac{1}{a} e_1^{1/a-1} e_1^1 - qe_1^1 - K_1|s|^{\rho_1}\text{sign}(s) - \omega \\ &= -e_1^2 - \lambda \frac{1}{a} \tilde{x}_1^{1/a-1} e_1^1 - qe_1^1 - K_1|s|^{\rho_1}\text{sign}(s) - \omega \end{aligned} \quad (13)$$

It can be indicated that the state is affected by both the dynamics of the sliding surface (7) and the observer error dynamics (6). In the following, we will prove that the observer error dynamics (6) cannot drive the sliding surface dynamics (7) and the state dynamics (6) to infinity within a finite time.

Combining (3) with (6), the observer estimation error is given by

$$\begin{aligned} \dot{e}_0^i &= -\lambda_0^i L_i^{\frac{1}{n-i+2}} |e_0^i|^{\frac{n-i+1}{n-i+2}} \text{sgn}(e_0^i) + e_1^i, \\ \dot{e}_j^i &= -\lambda_j^i L_i^{\frac{1}{n-i+2-j}} |e_j^i - \dot{e}_{j-1}^i|^{\frac{n-i+1-j}{n-i+2-j}} \text{sgn}(e_j^i - \dot{e}_{j-1}^i) + \dot{e}_{j+1}^i, \\ \dot{e}_{n-i+1}^i &\in -\lambda_{n-i+1}^i L_i \text{sgn}(e_{n-i+1}^i - \dot{e}_{n-i}^i) + [-L_i, L_i] \end{aligned} \quad (14)$$

where the estimation errors are defined as $e_0^i = z_0^i - x_i$, $e_j^i = z_j^i - d_i^{[j-1]}$. It follows from³³ that the observer error system (6) is finite-time stable, that is, Equation (14) indicates that regardless of the state x_i , the estimation error $e_i^j(t)$ will converge to zero within a finite time.

$$\begin{aligned} \dot{s} &= \dot{\tilde{x}}_2 + \lambda \left(\tilde{x}_1^{1/a} + q \right) (x_2 + \hat{d}_1) \\ &= \dot{\tilde{x}}_2 + \lambda \left(e_1^{1/a} + q \right) \tilde{x}_2 \end{aligned} \quad (15)$$

where $\tilde{x}_2 = \hat{x}_1 - \dot{x}_{1d} = x_2 + \hat{d}_1$. Then we can figure out as:

$$\dot{\tilde{x}}_2 = \lambda \left(e_1^{\frac{2}{a}} + q \right) \tilde{x}_2 - K_1 |s|^{\rho_1} \text{sign}(s) - K_2 \int_t^0 |s|^{\rho_2} \text{sign}(s) dt \quad (16)$$

$$\begin{cases} \dot{\xi}_1(t) = \rho_1 |\xi_1(t)|^{\frac{\rho_1-1}{\rho_1}} (-K_1(t)\xi_1(t) + \xi_2(t)) \\ \dot{\xi}_2(t) = -K_2(t) |\xi_1(t)|^{\frac{\rho_1-1}{\rho_1}} \xi_1(t) \end{cases} \quad (20)$$

Define a finite time bounded (FTB) function $V_1(s, x_1, \tilde{x}_2) = \frac{1}{2}(s^2 + x_1^2 + \tilde{x}_2^2)$ for the sliding mode dynamics (15) and the state dynamics (16). Note that $|s|^\rho < 1 + |s|$. Taking the derivative of V_1 :

$$\begin{aligned} \dot{V}_1 &= s\dot{\tilde{x}}_2 + \lambda \left(e_1^{\frac{2}{a}} + q \right) s\tilde{x}_2 + x_1(\tilde{x}_2 - e_1^1) + \dot{\tilde{x}}_2 \\ &= \lambda \left(e_1^{\frac{2}{a}} + q \right) s\tilde{x}_2 + x_1(\tilde{x}_2 - e_1^1) + (s + \tilde{x}_2) \\ &\quad \left(\lambda \left(e_1^{\frac{2}{a}} + q \right) \tilde{x}_2 - K_1 |s|^{\rho_1} \text{sign}(s) - K_2 \int_t^0 |s|^{\rho_2} \text{sign}(s) dt \right) \\ &= \lambda \tilde{x}_2 (2s + \tilde{x}_2) \left(e_1^{\frac{2}{a}} + q \right) + x_1(\tilde{x}_2 - e_1^1) - (s + \tilde{x}_2) (K_1 |s|^{\rho_1} \text{sign}(s) + K_2 \int_t^0 |s|^{\rho_2} \text{sign}(s) dt) \\ &\leq \lambda \left(e_1^{\frac{2}{a}} + q \right) (2|s||\tilde{x}_2| + \tilde{x}_2^2) + |x_1 x_2| + |x_1 e_1^1| \\ &\quad + (|s| + |\tilde{x}_2|)(K_1 |s| + K_2(1 + |s|)) \\ &\leq 2\lambda q \frac{\tilde{x}_2^2 + s^2}{2} + 2\lambda \left| e_1^{\frac{2}{a}} \right| \frac{\tilde{x}_2^2 + e_1^1}{2} + \frac{x_1^2 + \tilde{x}_2^2}{2} \\ &\quad + \frac{x_1^2 + (e_1^1)^2}{2} + (K_1 + K_2) \frac{\tilde{x}_2^2 + s^2}{2} \\ &\leq K_v V_1 + L_v \end{aligned} \quad (17)$$

where $K_v = \max\{2\lambda q + K_1 + K_2, 2\lambda q + K_1 + K_2 + 1 + 2\lambda |e_1^{\frac{2}{a}}|, 1\}$, and $L_v = \max\{\lambda(e_1^{\frac{2}{a}})^{\frac{1}{a}} + \frac{1}{2}(e_1^1)^2\}$ are bounded constants due to the boundedness of e_1^1 and e_1^2 . Since the disturbance estimation errors e_1^1 and e_1^2 in (14) will converge to zero in a finite time. Therefore, it can be concluded that system is finite-time stable. Theorem 1 completes the proof.

Proof 2. Due to the convergence of the perturbation estimation errors e_1^1 and e_1^2 to zero within a finite time as stated in equation (6), the system (13) can be simplified as:

$$\dot{s} = -K_1 |s|^{\rho_1} \text{sign}(s) - \omega \quad (18)$$

According to (8)–(18), letting $\bar{\omega} = -\omega$, we can derive a sliding mode system for each variable s_i with $i = \{\phi, \theta, \psi\}$ in the following manner:

$$\begin{cases} \dot{s}_i = -K_{1i} |s|^{\rho_1} \text{sign}(s) + \bar{\omega}_i \\ \dot{\bar{\omega}}_i = -K_{2i} |s|^{\rho_2} \text{sign}(s) \end{cases} \quad (19)$$

Letting $\xi(t) = [\xi_1(t), \xi_2(t)]^T$, $\xi_1(t) = |s(t)|^{\rho_1} \text{sign}(s(t))$ and $\xi_2(t) = \bar{\omega}$, we can get

Rewrite (20) as $\dot{\xi}(t) = M(t)\xi(t)$, where

$$M(t) = |\xi_1|^{\frac{\rho_1-1}{\rho_1}} \begin{bmatrix} -\rho_1 K_1 & \rho_1 \\ -K_2 & 0 \end{bmatrix}$$

A Lyapunov function is written as

$$V_{(\xi)}(t) = \xi^T(t) P \xi(t) \quad (21)$$

where

$$P = \begin{bmatrix} \theta + 4\epsilon^2 & -2\epsilon \\ -2\epsilon & 1 \end{bmatrix} \quad (22)$$

The derivative of the Lyapunov function is presented as

$$\begin{aligned} \dot{V}_{(\xi)}(t) &= \xi^T(t) (M^T P + P M) \xi(t) = -|\xi|^{\frac{\rho_1-1}{\rho_1}} \xi^T(t) \\ &\quad N(t) \xi(t) \end{aligned} \quad (23)$$

where

$$N(t) = \begin{bmatrix} N_{11}(t) & N_{12}(t) \\ N_{21}(t) & N_{22}(t) \end{bmatrix}$$

in which $N_{11}(t) = 2\rho_1 K_1 (\theta + 4\epsilon^2) - 4\epsilon K_2$, $N_{12}(t) = N_{21}(t) = -\rho_1 (\theta + 4\epsilon^2) - 2\rho_1 K_1 \epsilon + K_2$ and $N_{22}(t) = 4\rho_1 \epsilon$. The symmetric matrix $N(t)$ is positive definite with the minimal eigenvalue $\lambda_{\min}(N(t)) \geq 2\rho_1 \epsilon$ if

$$K_1 > \frac{2\epsilon + \rho_1 \epsilon}{\rho_1 \theta} + \frac{[\rho_1 (\theta + 4\epsilon^2)]^2}{4\rho_1^2 \epsilon \theta}$$

Therefore, one has that

$$\begin{aligned} \dot{V}_{(\xi)}(t) &\leq -|\xi_1|^{\frac{\rho_1-1}{\rho_1}} \xi^T(t) N(t) \xi(t) \\ &\leq -2\rho_1 \epsilon |\xi_1|^{\frac{\rho_1-1}{\rho_1}} \xi^T(t) \xi(t) \\ &= -2\rho_1 \epsilon |\xi_1|^{\frac{\rho_1-1}{\rho_1}} \|\xi(t)\|^2 \end{aligned} \quad (24)$$

We can see that

$$V_{(\xi)} \leq \lambda_{\max}(P) \|\xi(t)\|^2 \quad (25)$$

and

$$V_{(\xi)}^{\frac{1-\rho_1}{2\rho_1}} \geq \lambda_{\min}^{\frac{1-\rho_1}{2\rho_1}}(P) \|\xi(t)\|^{\frac{1-\rho_1}{\rho_1}} \quad (26)$$

According to (21)-(26), we can get

$$\dot{V}_{(\xi)} \leq -rV_{(\xi)}^{\varrho} \quad (27)$$

where $r = 2\rho_1 \epsilon^{\frac{1-\rho_1}{\lambda_{\min}^{2\rho_1}(P)}}$, $\varrho = \frac{3\rho_1-1}{2\rho_1} (\frac{1}{2} < \varrho < 1)$. There has a finite convergence time $t_f \leq \frac{1}{r(1-\varrho)} V_{(\xi)}^{1-\varrho}(0)$. Given that the adaptive law (10), the equation $K_1(t) \leq K_m + \omega_1 \sqrt{\frac{l_1}{2}} t_f$ is tenable. Set K_1^* and K_2^* as the maximum values of $K_1(t)$ and $K_2(t)$, respectively.

Considering the Lyapunov function

$$V_{(\xi, K)} = V_{(\xi)} + \frac{1}{2l_1} (K_1(t) - K_1^*)^2 + \frac{1}{2l_2} (K_2(t) - K_2^*)^2 \quad (28)$$

Let $\bar{K}_1(t) = K_1(t) - K_1^*$, $\bar{K}_2(t) = K_2(t) - K_2^*$, $V_{(K)}(t) = \dot{V}_{(\xi, K)}(t) - \dot{V}_{(\xi)}(t)$. According to (28), $V_{(K)}(t)$ becomes

$$\begin{aligned} V_{(K)}(t) &= \frac{1}{l_1} \bar{K}_1 \dot{K}_1 + \frac{1}{l_2} \bar{K}_2 \dot{K}_2 \\ &= -\frac{\omega_1}{\sqrt{2l_1}} |\bar{K}_1| - \frac{\omega_2}{\sqrt{2l_2}} |\bar{K}_2| + \frac{\omega_1}{\sqrt{2l_1}} |\bar{K}_1| \\ &\quad + \frac{\omega_2}{\sqrt{2l_2}} |\bar{K}_2| + \frac{1}{l_1} \bar{K}_1 \dot{K}_1 + \frac{1}{l_2} \bar{K}_2 \dot{K}_2 \end{aligned} \quad (29)$$

By Lemma 1, it is known that

$$\begin{aligned} rV_{(\xi)}^{\varrho}(t) + \frac{\omega_1}{\sqrt{2l_1}} |\bar{K}_1| + \frac{\omega_2}{\sqrt{2l_2}} |\bar{K}_2| \\ \geq rV_{(\xi)}^{\frac{1}{2}}(t) + \frac{\omega_1}{\sqrt{2l_1}} |\bar{K}_1| + \frac{\omega_2}{\sqrt{2l_2}} |\bar{K}_2| \\ \geq [r^2 V_{(\xi)}(t) + \left(\frac{\omega_1}{\sqrt{2l_1}}\right)^2 |\bar{K}_1|^2 + \left(\frac{\omega_2}{\sqrt{2l_2}}\right)^2 |\bar{K}_2|^2]^{\frac{1}{2}} \end{aligned} \quad (30)$$

Letting $\Lambda = \min\{\omega_1, \omega_2, r\}$, we can get

$$\begin{aligned} rV_{(\xi)}^{\frac{1}{2}}(t) + \frac{\omega_1}{\sqrt{2l_1}} |\bar{K}_1| + \frac{\omega_2}{\sqrt{2l_2}} |\bar{K}_2| \\ \geq \Lambda [V_{(\xi)} + \left(\frac{1}{\sqrt{2l_1}}\right)^2 |\bar{K}_1|^2 + \left(\frac{1}{\sqrt{2l_2}}\right)^2 |\bar{K}_2|^2]^{\frac{1}{2}} \\ = \Lambda \sqrt{V_{(\xi, K)}(t)} \end{aligned} \quad (31)$$

According to the (27), (29), and (31), we can get

$$\dot{V}_{(\xi, K)}(t) \leq -\Lambda \sqrt{V_{(\xi, K)}(t)} + \bar{V}_{(K)}(t) \quad (32)$$

where

$$\begin{aligned} \bar{V}_{(K)}(t) &= \frac{1}{l_1} \bar{K}_1(t) \dot{K}_1(t) + \frac{1}{l_2} \bar{K}_2(t) \dot{K}_2(t) \\ &\quad + \frac{\omega_1}{\sqrt{2l_1}} |\bar{K}_1(t)| + \frac{\omega_2}{\sqrt{2l_2}} |\bar{K}_2(t)| \\ &= -|\bar{K}_1(t)| \left(\frac{1}{l_1} \dot{K}_1(t) - \frac{\omega_1}{\sqrt{2l_1}} \right) \\ &\quad - |\bar{K}_2(t)| \left(\frac{1}{l_2} \dot{K}_2(t) - \frac{\omega_2}{\sqrt{2l_2}} \right) \end{aligned} \quad (33)$$

Then, an analysis of the sign of $\bar{V}_{(K)}(t)$ is conducted, leading to an examination of the sign of the time derivative of the Lyapunov function. To ensure the stability of $\dot{V}_{(\xi, K)}(t)$, two cases are considered.

Case 1. Assume that $K_1(t) > K_m$ and $|s| > \mu$. Afterwards, $K_1(t)$ is raised until the sliding mode emerges. Let $\epsilon = \frac{\omega_2}{2\rho_1\omega_1} \sqrt{\frac{l_2}{l_1}}$, we can get that $\bar{V}_{(K)}(t) = 0$ and $\dot{V}_{(\xi, K)}(t) \leq -\Lambda \sqrt{V_{(\xi, K)}(t)}$. Then, the convergence of the sliding mode to the domain $|s| \leq \mu$ is guaranteed within a finite time t_f .

Case 2. Suppose that $|s| < \mu$, that means $K_1(t)$ will reduce in according to (10). The term $\bar{V}_{(K)}(t)$ satisfies the following two conditions:

$$\bar{V}_{(K)}(t) = \begin{cases} 2|K_1 - K^*| \frac{\omega_1}{\sqrt{2l_1}}, & \text{if } K_1(t) > K_m \\ -|K_m + \eta t - K^*| \left(\frac{\eta}{l_1} - \frac{\omega_1}{\sqrt{2l_1}} \right), & \text{if } K_1(t) \leq K_m \end{cases} \quad (34)$$

We can see that the term $\bar{V}_{(K)}(t)$ relies on the value of $K_1(t)$. When $K_1(t)$ is smaller than K_m , the term $\bar{V}_{(K)}(t)$ is negative. Then, we can obtain that $\bar{V}_{(K)}(t) \leq 0$ and $\dot{V}_{(\xi, K)}(t) \leq -\Lambda \sqrt{V_{(\xi, K)}(t)}$. As a result, the sliding mode will converge within a finite time. Once $K_1(t)$ exceeds K_m , the term $\bar{V}_{(K)}(t)$ becomes positive, causing the sign of the Lyapunov function (28) to become indefinite, and $|s|$ might exceed the range of μ . In such a scenario, **Case 1** applies to ensure $|s| < \mu$ again. It implies that $K_1(t)$ should increase according to (10) to ensure that $\bar{V}_{(K)}(t)$ remains negative definite.

Simulation

In this section, Figure 2 depicts the block diagram of the observer-based ASTFTSMC for the quadrotor UAV system. MATLAB/Simulink software is utilized for simulation to demonstrate the effectiveness of the proposed method. Firstly, robustness analysis is conducted on ASTFTSMC and compared with ASTSMC. Then, we compared the performance of proposed method with other approaches when only matched disturbances are present and when both matched and mismatched disturbances are present.

Table 1. Body parameters of the quadrotor UAV.

Parameter	Description	Value	Unit
m	Mass	2.85	Kg
l	Distance	0.1969	m
K_f	Thrust factor	2.98e-6	N/V
K_t	Drag factor	1.14e-7	
J_{xx}	Roll inertia ϕ	0.0552	kgm ²
J_{yy}	Pitch inertia θ	0.0552	kgm ²
J_{zz}	Yaw inertia ψ	0.1104	kgm ²

Table 1 lists the selected physical parameters for the UAV refer to Kahouadji et al.²³ The parameter ρ_1 of the developed controller is chosen as 0.8.

Desired trajectory tracking with external disturbances

This section focuses on the robustness analysis of the proposed method and compares the results to ASTSMC. The parameters of the sliding surface are chosen as $\lambda = [8, 8, 8]$, $a = [\frac{9}{11}, \frac{9}{11}, \frac{9}{11}]$, $q = [5, 2, 1]$. The ASTSMC parameters are chosen as $\omega_{1i} = 6, l_{1i} = 2, \mu_i = 0.05, K_{mi} = 0.8, \eta = 0.8, \epsilon = 1, \dot{K}_1(0) = [3, 2, 3]$. The controller parameters are chosen as $\omega_{1i} = 6, l_{1i} = 2, \mu_i = 0.05, K_{mi} = 0.8, \eta = 0.8, \epsilon = 0.1, \dot{K}_1(0) = [6, 8, 8]$. The reference signals are selected as $\phi_d = \sin(t), \theta_d = \cos(t), \psi_d = \sin(t)$. The initial states are set $\phi_0 = 1, \theta_0 = 0.5, \psi_0 = 1$. The external time-varying disturbances are given by $d_{2\phi} = d_{2\theta} = d_{2\psi} = \sin(t)$, where

$$a = \begin{cases} 0, & t < 10 \\ 0.1, & 10 \leq t < 20 \\ 0.5, & 20 \leq t \end{cases}$$

Figure 3 shows the performance tracking of quadrotor attitude. we can see that three attitude angles reach their references more quickly and accurately. Figure 4 depicts the adaptive parameter $K_1(t)$ of ASTFTSMC.

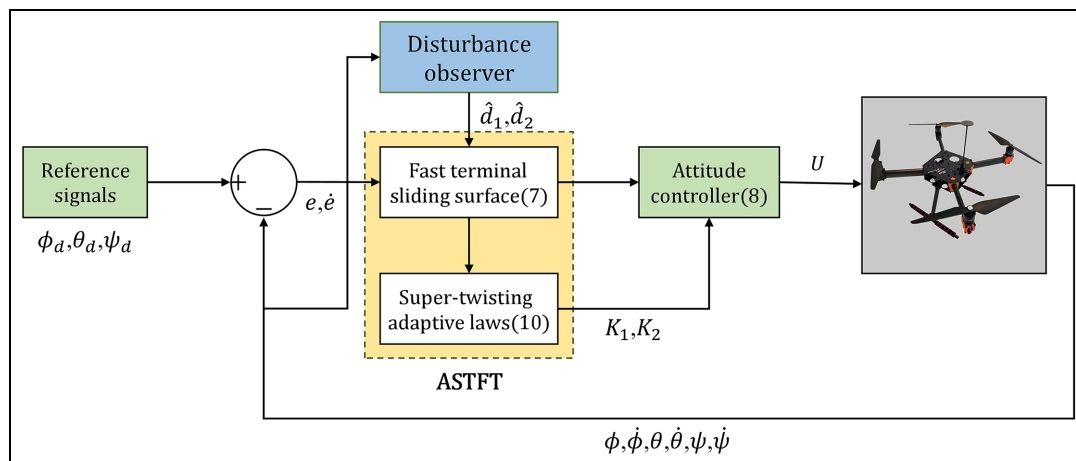
From 10 to 20ss, smaller disturbances are associated with lower gains, while after 20s, gains increase with growing disturbances to ensure the sliding surface converges within the $\bar{\mu}$ range. This validates the effectiveness of the adaptive law. In conclusion, the simulation results demonstrate the feasibility and superiority of the proposed method.

Comparative study

Case 1. In this part, a comparison with adaptive super-twisting non-singular terminal sliding mode controller (ASTNTSMC) proposed in Khodadadi and Ghadiri¹ is introduced to demonstrate the superiority of the proposed method. The initial states are set $\phi_0 = 0, \theta_0 = 0.1, \psi_0 = 0.1$. The reference signals are selected as $\phi_d = 0.1 \cos(t), \theta_d = 0.1 \sin(t), \psi_d = 0.1 \sin(t)$. The parameters of the observer are chosen as $\lambda_0^1 = 10, \lambda_0^2 = 5, \lambda_1^1 = 10, \lambda_1^2 = 3, \lambda_2^1 = 1, L_1 = 1, L_2 = 1$. The parameters of the controller are chosen as $\lambda = [10, 10, 10], a = [\frac{9}{11}, \frac{9}{11}, \frac{9}{11}], q = [5, 3, 4], \omega_{1i} = 6, l_{1i} = 2, \mu_i = 0.05, K_{mi} = 0.8, \eta = 0.8, \epsilon = 0.1, \dot{K}_1(0) = [3.5, 5, 5.5]$. The disturbances are given by $d_{2\phi} = d_{2\theta} = d_{2\psi} = 0.01 \sin(4 \times t)$.

Figures 5 and 6 display the comparison of the tracking performance and control inputs between two methods. In Figure 5, the results indicate that the proposed method is capable of tracking attitude more quickly and accurately. In Figure 6, we can observe that while ASTNTSMC is represented by the blue oscillatory trajectory, the controller proposed in this paper is represented by the red smooth trajectory. This indicates that the controller in this paper significantly reduces the chattering effect by generating smooth and continuous control signals.

Case 2. In this part, the matched disturbances are given by $d_{2\phi} = d_{2\theta} = d_{2\psi} = 0.05 \cos(t)$, and the mismatched disturbances are given by $d_{1\phi} = d_{1\theta} = d_{1\psi} = 0.05 \sin(t)$, the rest of parameters are selected the same as in

**Figure 2.** Block diagram of the observer-based ASTFTSMC controller.

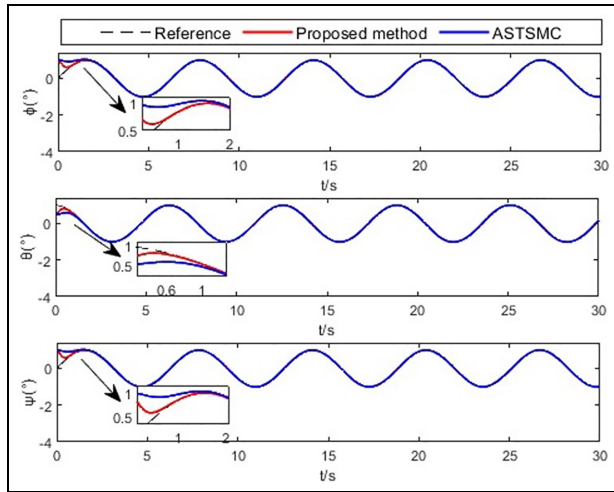


Figure 3. Altitude tracking of quadrotor UAV.

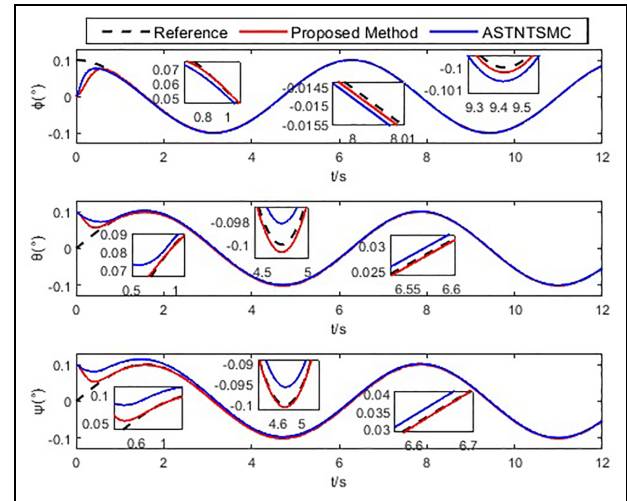


Figure 5. Comparison of attitude tracking.

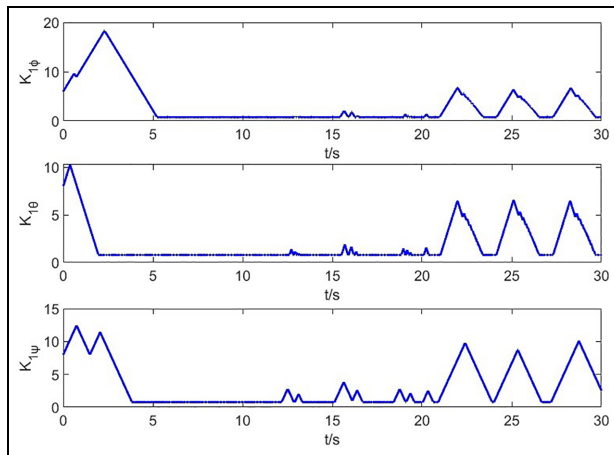


Figure 4. Adaptive gains by ASTFTSMC.

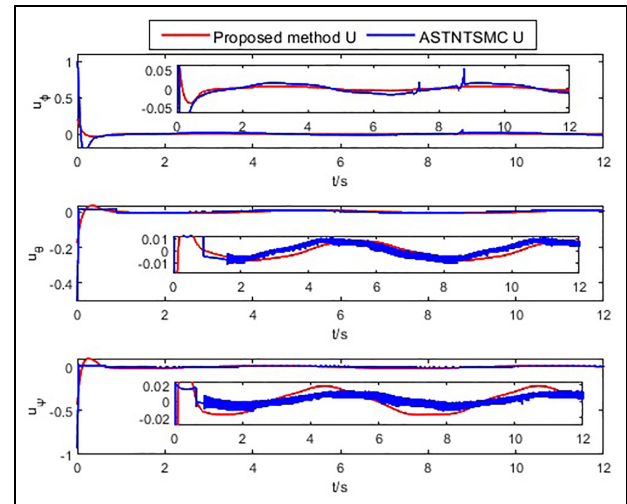


Figure 6. Comparison of control signals.

case 1. In Figure 7, the results demonstrate that the controller proposed in¹ exhibits limited effectiveness in controlling the UAV system subject to mismatched disturbances. Clearly, our proposed method is capable of tracking attitude more quickly and accurately. This further validates the robustness and effectiveness of the proposed approach.

To provide a clearer comparison between ASTNTSMC proposed in Khodadadi and Ghadiri¹ and the proposed method, four performance evaluation metrics from Tables 2 and 3 are used, with the average values of the three attitude angles computed for evaluation. The first performance metric is Mean Squared Error (MSE), which measures the proximity between the tracking results and the desired values. In the proposed method, the MSE decreases in Case 1 when only matched disturbances are present, and it decreases even more significantly in Case 2 when both matched and mismatched disturbances are present. The second metric is Error Variance (EV), which measures the variability of the errors. It represents the average

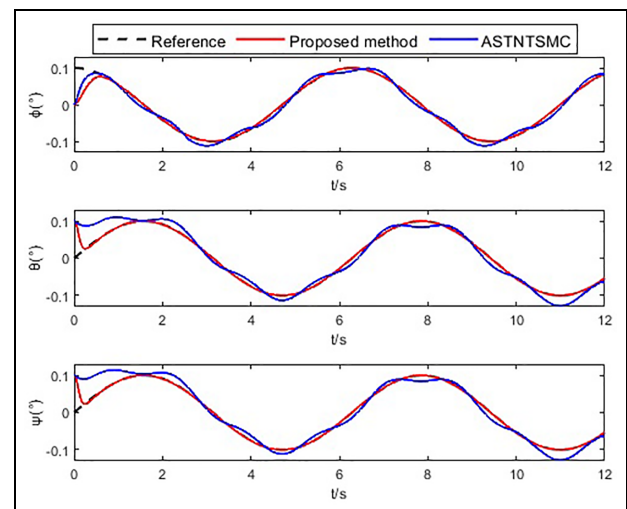


Figure 7. Comparison of attitude tracking with mismatched disturbances.

Table 2. The performance evaluation metrics of the designed controller in comparison to other methods in case 1.

performance evaluation metrics	Formula	ASTNTSMC	Proposed method
Mean Square Error (MSE)	$MSE = \frac{1}{T} \sum_{t=1}^T [x_{di} - x_i]^2$	1.715e-04	1.408e-04
Error Variance (EV)	$\sigma_e^2 = \frac{\sum_{i=1}^N (e_i - \mu_e)^2}{N}$	1.429e-04	1.372e-04
Integral of Square Error (ISE)	$ISE = \int_0^T e^2(t) dt$	2.054	1.685
Integral of Absolute Error (IAE)	$IAE = \int_0^T e(t) dt$	58.281	30.494

Table 3. The performance evaluation metrics of the designed controller in comparison to other methods in case 2.

performance evaluation metrics	Formula	ASTNTSMC	Proposed method
Mean Square Error (MSE)	$MSE = \frac{1}{T} \sum_{t=1}^T [x_{di} - x_i]^2$	3.180e-04	9.980e-05
Error Variance (EV)	$\sigma_e^2 = \frac{\sum_{i=1}^N (e_i - \mu_e)^2}{N}$	3.082e-04	9.778e-05
Integral of Square Error (ISE)	$ISE = \int_0^T e^2(t) dt$	3.811	1.193
Integral of Absolute Error (IAE)	$IAE = \int_0^T e(t) dt$	141.665	20.258

deviation of the actual values from their expected values, indicating the level of dispersion. A smaller error variance indicates that the actual values are closer to their expected values, implying higher accuracy and stability of the system. It can be observed that in both cases, the proposed method in this paper leads to a reduction in error variance. In fact, minimizing error is the core objective in any input control system. The third metric, Integral of Squared Error (ISE), and the fourth metric, Integral of Absolute Error (IAE), are defined by integrating the area under the tracking error curve. A smaller value for these metrics indicates a smaller tracking error and better performance of the control system. In the proposed method, both of these metrics show a significant reduction.

Conclusion

This paper proposes an ASTFTSMC based on observer for the attitude tracking control of quadrotor UAVs considering the unknown mismatched disturbances. For this purpose, a dynamic adaptive gain is proposed to reduce the chattering effect. Additionally, a fast terminal adopting observer SMC scheme is proposed, which effectively addresses the challenges caused by mismatched disturbances while improving convergence speed. The simulation results demonstrate the effectiveness of the proposed method.

The development goals and future prospects of this research are multifaceted. Firstly, further development can be done to create a control method with fewer control parameters, through techniques such as parameter integration and optimization, to reduce the chattering effort. Secondly, while this study focuses on attitude control of quadrotor UAVs, future research can take a comprehensive approach, including position control

and path planning, to enhance the control performance and application range of UAVs, catering to the needs of real-world applications. Furthermore, this research has not been validated through physical implementation. Future research can include experimental validation to provide more accurate guidance and evaluation for optimizing and improving the control method, and to facilitate the practical implementation and dissemination of the proposed control approach.


Declaration of conflicting interests

The author(s) declared no potential conflicts of interest with respect to the research, authorship, and/or publication of this article.

Funding

The author(s) disclosed receipt of the following financial support for the research, authorship, and/or publication of this article: This research is financially supported by the National Natural Science Foundation of China (Grant No.62273254).

ORCID iD

Shanshan Zhang  <https://orcid.org/0009-0008-3086-5802>

References

1. Khodadadi H and Ghadiri H. Adaptive super-twisting non-singular terminal sliding mode control for tracking of quadrotor with bounded disturbances. *Aero Sci Technol* 2021; 112(1): 106616.
2. Hien NV and Diem PG. *A model-based design to implement controllers for quadrotor unmanned aerial vehicles*. World Scientific and Engineering Academy and Society, 2019.

3. Idrissi M, Salami M and Annaz F. A review of quadrotor unmanned aerial vehicles: applications, architectural design and control algorithms. *Journal of Intelligent and Robotic Systems* 2022; 104(2): 1–33.
4. Mao JH. *Application of aerial surveying technology of low altitude light uav in mine topographic surveying and mapping*. World Nonferrous Metals 2018.
5. Mohtasin G, Lee JM and Kim DS. Enhancement of security constraints in uav-assisted iot deployment using blockchain technology in military operations. *Korean Communication Society Academic Conference Proceedings Collection*, Pyeongchang, Gangwon Province, Korea 2020; pp. 479–480.
6. Ajith VS and Jolly KG. Unmanned aerial systems in search and rescue applications with their path planning: a review. *J Phys Conf Ser* 2021; 2115(1): 012020.
7. Cao Y, Cheng X and Mu J. Concentrated coverage path planning algorithm of UAV formation for aerial photography. *IEEE Sen J* 2022; 22(11): 11098–11111.
8. Motlagh NH, Kortocxi P, Su X, et al. Unmanned aerial vehicles for air pollution monitoring: a survey. *IEEE Internet of Things Journal* 2023; 10(24): 21687–21704.
9. Han B and Fang S. A frame model of power pylon detection for UAV-based power transmission line inspection. *Zhejiang Elect Power* 2016; 35(4): 6–11.
10. Furlanetto RH, Rafael NM and Guilherme L. Identification and quantification of potassium (K +) deficiency in maize plants using an unmanned aerial vehicle and visible/near-infrared semi-professional digital camera. *Int J Rem Sens* 2021; 42(23): 8783–8804.
11. Liu W, Cheng X and Zhang J. Command filter-based adaptive fuzzy integral backstepping control for quadrotor UAV with input saturation. *J Franklin Inst* 2023; 360(1): 484–507.
12. Rekabi F, Shirazi FA, Sadigh MJ, et al. Nonlinear H_∞ measurement feedback control algorithm for quadrotor position tracking. *J Franklin Inst* 2020; 357(11): 6777–6804.
13. Li C, Wang Y and Yang X. Adaptive fuzzy control of a quadrotor using disturbance observer. *Aerospace Sci Technol* 2022; 128: 107784.
14. Utkin V. Variable structure systems with sliding modes. *IEEE Transact Autom Cont* 1977; 22(2): 212–222.
15. Behera PK, Mendi B, et al. Robust wind turbine emulator design using sliding mode controller. *Ren Energy Focus* 2021; 36(3): 79–88.
16. Benaddy A, Labbadi M and Bouzi M. Robust flight control for a quadrotor under external disturbances based on generic second order sliding mode control. *IFAC-PapersOnLine* 2022; 55(12): 270–275.
17. Chen L, Liu Z, Dang Q, et al. Robust trajectory tracking control for a quadrotor using recursive sliding mode control and nonlinear extended state observer. *Aerospace Sci Technol* 2022; 128: 107749.
18. Nettari Y, Kurt S and Labbadi M. Adaptive Robust Control based on Backstepping Sliding Mode techniques for Quadrotor UAV under external disturbances. *IFAC-PapersOnLine* 2022; 55(12): 252–257.
19. Guo GX, An XH, et al. Observer-based event-triggered sliding mode tracking control for uncertain robotic manipulator systems. *J Braz Soc Mech Sci Eng* 2023; 45(9): 453.
20. Singh P, Giri DK and Ghosh AK. Robust backstepping sliding mode aircraft attitude and altitude control based on adaptive neural network using symmetric BLF. *Aerospace Sci Technol* 2022; 126: 107653.
21. Levant A. Sliding order and sliding accuracy in sliding mode control. *Int J Cont* 1993; 58(6): 1247–1263.
22. Derafa L, Benallegue A and Fridman L. Super twisting control algorithm for the attitude tracking of a four rotors UAV. *J Franklin Instit* 2012; 349(2): 685–699.
23. Kahouadji M, Mokhtari MR, Choukchou BA, et al. Real-time attitude control of 3 DOF quadrotor UAV using modified super twisting algorithm. *J Franklin Inst* 2020; 357(5): 2681–2695.
24. Razmi H and Afshinfar S. Neural network-based adaptive sliding mode control design for position and attitude control of a quadrotor UAV. *Aerospace Sci Technol* 2019; 91: 12–27.
25. Abdulraheem KK, Tolokonsky AO and Laidani Z. Adaptive second-order sliding-mode control for a pressurized water nuclear reactor in load following operation with Xenon oscillation suppression. *Nucl Eng Des* 2022; 391: 111742.
26. Abhinav K and Kumar SR. Modified super-twisting sliding mode-based control design for robust hovering of quadrotor. *IFAC-PapersOnLine* 2022; 55(22): 135–140.
27. Xu LX, Wang YL, Wang F, et al. Event-triggered active disturbance rejection trajectory tracking control for a quadrotor unmanned aerial vehicle. *Appl Math Comp* 2023; 449: 127967.
28. Negrete DY and Moreno JA. Second-order sliding mode output feedback controller with adaptation. *Int J Adap Cont Sig Process* 2016; 30(8–10): 1523–1543.
29. Shtessel Y, Taleb M and Plestan F. A novel adaptive-gain supertwisting sliding mode controller: methodology and application. *Automatica* 2012; 48(5): 759–769.
30. Moghaddam RK, Mohamadie NK, et al. Fast terminal nonsingular sliding mode control of wave energy converters for maximum power absorption. *Ocean Eng* 2023; 281: 114473.
31. Xu DH, Liu ZP, et al. Trajectory tracking of underactuated unmanned surface vessels: non-singular terminal sliding control with nonlinear disturbance observer. *Appl Sci* 2022; 12(6): 3004.
32. Luo WL and Liu S. Disturbance observer based nonsingular fast terminal sliding mode control of underactuated AUV. *Ocean Eng* 2023; 279: 114553.
33. Yang J, Li SH, et al. Continuous nonsingular terminal sliding mode control for systems with mismatched disturbances. *Automatica* 2013; 49: 2287–2291.
34. Nguyen NP, Oh H, Moon J, et al. Multivariable disturbance observer-based finite-time sliding mode attitude control for fixed-wing UAVs under matched and mismatched disturbances. *IEEE Control Systems Letters* 2023; 279: 114553.
35. Labbadi M and Cherkaoui M. Robust adaptive nonsingular fast terminal sliding-mode tracking control for an uncertain quadrotor UAV subjected to disturbances. *ISA Transact* 2020; 99: 290–304.
36. Lei W, Li C and Chen MZ. Robust adaptive tracking control for quadrotors by combining PI and self-tuning regulator. *IEEE Transact Cont Sys Technol* 2018; 27(6): 2663–2671.